STRUCTURE CHARACTERISTIC FOR TEMPERATURE FLUCTUATIONS AND THE OUTER SCALE OF ATMOSPHERIC TURBULENCE RECONSTRUCTED FROM THE DATA OF ACOUSTIC SOUNDING

N.P. Krasnenko and L.G. Shamanaeva

Institute of Atmospheric Optics,
Siberian Branch of the Russian Academy of Sciences, Tomsk
Received August 19, 1997

Profiles of the structure characteristic for temperature fluctuations C_T^2 and the outer scale of atmospheric turbulence L_0 are reconstructed from the data of acoustic sounding with the Zvuk–2 three-channel Doppler sodar. An iterative algorithm considering the turbulent signal attenuation is used for sodar data interpretation. A comparison between sodar derived C_T^2 and in situ measurements with micropulsation sensors demonstrates their good agreement. For the first time, vertical profiles of the outer scale of atmospheric turbulence have been obtained for the atmospheric boundary layer. Sodar derived L_0 agree well with the estimates of the effective outer scale of turbulence by optical methods.

Nowadays acoustic radars (sodars) are widely used to measure the profiles of structure characteristics for temperature fluctuations in the atmospheric boundary layer. However, a comparison of sodar data with *in situ* measurements shows that the standard deviation of sodar data reaches 40% at altitudes 30–500 m. Their maximum discrepancy may reach a factor of 2–5. We believe that a possible reason for the discrepancy is neglect of the turbulent attenuation of a sodar signal when it propagates to a sounded volume and back to a receiver. In the present paper, the interpretation of sodar data is performed with the use of an iterative algorithm[1–3] considering the turbulent signal attenuation. This allows the vertical profiles of the outer scale of atmospheric turbulence to be obtained.

The outer scale of turbulence plays an important role in the theory of turbulence, because it defines the low-frequency boundary of the inertial subrange in the spectra of temperature and wind velocity fluctuations.[4] Knowledge of L_0 is necessary for estimating the turbulent attenuation of a sound wave.[5] Nevertheless, the vertical profiles of L_0 have never been measured in the atmospheric boundary layer, although Sazarin[6] point out their strong dependence on local orography.

In the present paper, we discuss the vertical profiles of the structure characteristic for temperature fluctuations C_T^2 and the outer scale of atmospheric turbulence L_0 measured with the Zvuk–2 three-channel Doppler sodar. Regular measurements have been performed since August 1996. Sodar specifications are given below.

Vertical sensing range, m	40–700
Operating frequency f, Hz	1650–1850
Electrical transmitted power P_0, W	65
Pulse repetition period Δt, s	4, 6, 12
Pulse duration τ, ms	150
Effective transceiving antenna area A_{eff}, m^2	0.5
Efficiency of conversion of electrical power into acoustic power and *vice versa*, $\gamma_1 = \gamma_2$	0.1

The structure characteristic of temperature fluctuations is calculated by the formula

$$C_T^{2(j)}(z_i) = \frac{2.7 \cdot 10^2 \, \lambda^{1/3} \, T^2 \, P(z_i) \, z_i^2}{\gamma_1 \, \gamma_2 \, P_0 \, c \, A_{\text{eff}} \, \tau \, L^{(j-1)}(z_i)} , \qquad (1)$$

where j is the iteration number, $j = 1,\ldots, M$; z_i is the current altitude of the sounded volume, $z_i = i\Delta z$, $\Delta z = c\tau/2$ is the altitude resolution of the sodar, $i = i_0$, $i_0 + 1,\ldots, N$; i_0 specifies the minimum sounding altitude $z_0 = i_0 \Delta z$, N specifies the maximum sounding altitude and is equal to the number of range gates in the realization; c is the sound speed in air, $c = 20.05\sqrt{T}$; T is the surface air temperature; $\lambda = c/f$ is the acoustic radiation wavelength; $P(z_i)$ is the power of the acoustic signal coming from the altitude z_i;

$$L^{(j)}(z_i) = L_{\text{abs}}(z_i) \, L_{\text{turb}}^{(j)}(z_i) \qquad (2)$$

is the attenuation factor considering the signal attenuation on the propagation path to the sounded volume and back to the receiver caused by the classical and molecular absorption $L_{\text{abs}}(z_i)$ and by the turbulent

0235-6880/98/01 60-06 $02.00

attenuation $L_{\text{turb}}^{(j)}(z_i)$ due to scattering by temperature and wind velocity fluctuations.

The first iteration $C_T^{2(1)}(z)$ was calculated from Eq. (1) without turbulent attenuation for

$$L^{(0)}(z_i) = L_{\text{abs}}(z_i) = \exp\{-2\,(\beta_{\text{cl}} + \beta_{\text{mol}})\, z_i\}. \quad (3)$$

In so doing, the classical and molecular absorption coefficients were calculated by the formulas[7]

$$\beta_{\text{cl}}(f) = 4.02\cdot 10^{-11}\, f^2, \ [\text{m}^{-1}], \quad (4)$$

$$\beta_{\text{mol}}(f,t,u) = \frac{\beta_{\max}}{304.8}\left[(0.18 f_{\text{k}})^2 + \left(\frac{2 f_{\text{k}}^2}{1+f_{\text{k}}}\right)^2\right]^{1/2}, \ [\text{m}^{-1}], \quad (5)$$

where $f_{\text{k}} = f/f_{\text{m}}$, f_{m} is the frequency at which the maximum absorption occurs at the given temperature t[°C], pressure p[mbar], and relative humidity u[%], determined from the formula

$$f_{\text{m}} = (10 + 6600\, h + 444000\, h^2)\, p_1 / t_1^{0.8}. \quad (6)$$

Here, the normalized pressure $p_1 = p/1014$, $t_1 = (1.8t + 492)/519$, and the parameter $h = e_1\cdot 100/p_1$ depends on the water vapor pressure e_1 in the atmosphere which is given by the formula[8]

$$e_1 = 0.0611107\cdot 10^{M_1}\cdot u \quad (7)$$

with

$$M_1 = 7.63\, t/(241.9 + t)\ . \quad (8)$$

Then the parameter $\beta_{\max}$ in Eq. (5) is calculated from the relation

$$\beta_{\max} = 0.0018\, t_1^{-2.5} \exp\{7.77\,(1 - t_1^{-1})\}\ . \quad (9)$$

The second and the next iterations of C_T^2 were calculated considering the turbulent attenuation. The turbulent attenuation factor in Eq. (2) (for the jth iteration) was calculated by the formula

$$L_{\text{turb}}^{(j)}(z_i) = \exp\left\{-2\,\Delta z \sum_{i=1}^{N} [\beta_V^{(j)}(z_i) + \beta_T^{(j)}(z_i)]\right\}. \quad (10)$$

Here, the coefficients of scattering by the temperature and wind velocity fluctuations were calculated by the formulas

$$\beta_V^{(j)}(z_i) = 9.545\,\frac{C_V^2(z_i)}{c^2}\,\frac{[L_0^{(j)}(z_i)]^{5/3}}{\lambda^2}\ , \quad (11)$$

$$\beta_T^{(j)}(z_i) = 0.3596\,\frac{C_T^{2(j)}(z_i)}{T^2}\,\frac{[L_0^{(j)}(z_i)]^{5/3}}{\lambda^2}\ , \quad (12)$$

derived in Ref. 5 for $L_0^2 \gg \lambda^2$, which is satisfied in our case ($\lambda = 20$ cm). The jth iteration of C_T^2 entering Eq. (12) was calculated by Eq. (1).

The outer scale of atmospheric turbulence and the structure characteristic of wind velocity fluctuations were determined as follows.

The structure characteristics of the wind velocity fluctuations were determined by averaging of the instantaneous wind velocity components $V_{x_k}(z_i)$, $V_{y_k}(z_i)$, and $V_{z_k}(z_i)$ measured by the Zvuk–2 sodar

$$C_V^2(z_i) = \left(\Delta t\sqrt{V_{x\,\text{av}}^2(z_i) + V_{y\,\text{av}}^2(z_i) + V_{z\,\text{av}}^2(z_i)}\right)^{-2/3} \times$$

$$\times\,\frac{1}{K-1}\sum_{k=1}^{K-1}[V_k(z_i) - V_{k+1}(z_i)]^2, \quad (13)$$

where $\Delta t = 12$ s is the sound pulse repetition period, $M = 50$ is the number of pulses in a measurement series,

$$V_{x\,\text{av}}(z_i) = \frac{1}{K}\sum_{k=1}^{K} V_{x_k}(z_i),\ V_{y\,\text{av}}(z_i) = \frac{1}{K}\sum_{k=1}^{K} V_{y_k}(z_i),$$

$$V_{z\,\text{av}}(z_i) = \frac{1}{K}\sum_{k=1}^{K} V_{z_k}(z_i) \quad (14)$$

are the components of the wind velocity averaged over the period $K\Delta t$, and

$$V_k(z_i) = \frac{V_{x_k}(z_i)\,V_{x\,\text{av}}(z_i) + V_{y_k}(z_i)\,V_{y\,\text{av}}(z_i) + V_{z_k}(z_i)\,V_{z\,\text{av}}(z_i)}{\sqrt{V_{x\,\text{av}}^2(z_i) + V_{y\,\text{av}}^2(z_i) + V_{z\,\text{av}}^2(z_i)}}. \quad (15)$$

Because in our experiment we measured only the wind velocity components averaged over 10-min intervals, C_V^2 was approximated by the relation

$$C_V^2(z_i) = C_{V_0}\,(0.04 + 0.33\, z_i^{-2/3}) \qquad (16)$$

suggested in Ref. 9 for the daytime convection. The parameter C_{V_0} was determined from the data of *in situ* measurements performed by micropulsation sensors placed 17 m above the ground.

The outer scale of atmospheric turbulence was estimated as follows. At visible wavelengths, Tatarskii[10] derived the expression for the structure characteristic of the refractive index

$$C_n^2(z_i) = 2.8\, M(z)\, L_0^{4/3}(z), \qquad (17)$$

where $M(z)$ is the potential refractive index gradient related with the gradient of the potential temperature logarithm by the formula

$$M(z) = -\,78 \cdot 10^6\, \frac{p(z)}{T(z)}\, \frac{\delta \ln \theta(z)}{\delta z}\,. \qquad (18)$$

In its turn, the potential temperature is defined by the air temperature and pressure

$$\theta(z) = T(z)\, [1000/p(z)]^{0.286}. \qquad (19)$$

According to the formula[11]

$$C_n^2(z) = C_T^2(z) \left[\frac{78 \cdot 10^6\, p(z)}{T^2(z)}\right]^2, \qquad (20)$$

the structure characteristic of the refractive index at visible wavelengths is connected with the structure characteristic of the temperature fluctuations, so from Eqs. (17)–(19) we derive

$$L_0(z) = \left[\frac{C_T^2(z)}{2\,[\delta\theta/\delta z]^2} \left(\frac{p(z)}{1000}\right)^{0.572}\right]^{3/4}. \qquad (21)$$

For the atmospheric boundary layer at altitudes $40 \le z \le 700$ m, we can take $p(z) \cong 1000$ mbar, $\delta\theta/\delta z \cong \gamma_a$ (see Ref. 12), where γ_a is the adiabatic temperature gradient. Finally, for the jth iteration of the outer scale of atmospheric turbulence we obtain

$$L_0^{(j)}(z_i) = [C_T^{2(j)}(z_i)/(2.8\, \gamma_a^2)]^{3/4}. \qquad (22)$$

The iterative algorithm of acoustic sounding data processing was constructed in the following way. The structure characteristic of temperature fluctuations was calculated by Eq. (1) and the outer scale of atmospheric turbulence – by Eq. (22) sequentially for each strobe pulse $i = i_0,\ i_0 + 1,\ \ldots,\ N$. The minimum sounding altitude $z_0 = i_0 \Delta z$ was determined by the sodar dead zone and environmental noise level and changed from 66 to 88.5 m as a function of meteorological conditions and surrounding noise level. The maximum sounding altitude changed from 250 to 650 m. For each strobe pulse starting from i_0 the first iteration $C_T^{2(1)}$ was calculated without turbulent attenuation. Then the first iteration of the outer scale of turbulence $L_0^{(1)}$ was calculated by Eq. (22). Its value was used to calculate the first iterations of the attenuation coefficients by Eqs. (11) and (12). It was substituted into Eq. (10) to calculate the first iteration of the turbulent attenuation factor which was further substituted into Eq. (1) to calculate the second iteration $C_T^{2(2)}(z_i)$, and so on. The iteration process terminated when the number of iterations exceeded 100 or when the next iterations started to diverge.

Figure 1 shows the facsimile record of the Zvuk–2 sodar operated on September 29, 1996 under conditions of developed convection. Intensive thermal plumes up to 120–200 m can be seen. The arrows indicate times of starting of three subsequent 10-min runs; the corresponding vertical profiles of C_T^2 are shown in Fig. 2.

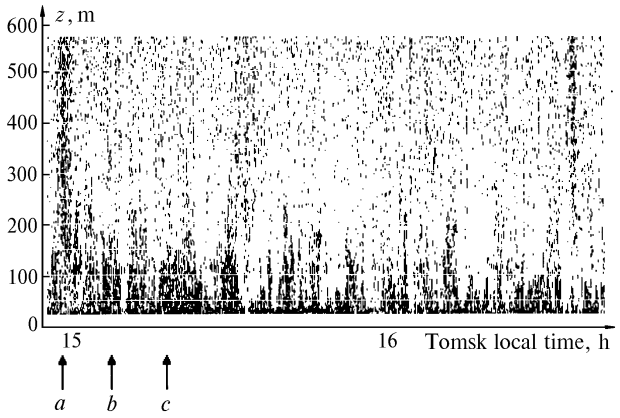

FIG. 1. The facsimile record of the Zvuk–2 sodar operated on September 29, 1996 from 14:55 to 16:47, Tomsk local time. The arrows indicate times of starting of three subsequent runs; their data were processed with the use of the proposed iterative algorithm.

For comparison, Fig. 3 shows the vertical profiles of C_T^2 reconstructed from the data of acoustic sounding in the morning under conditions of developing convection. The structure characteristics were normalized to $C_T^2\ (z_0)$ measured at the minimum sounding altitude. Their numerical values are indicated near the curves.

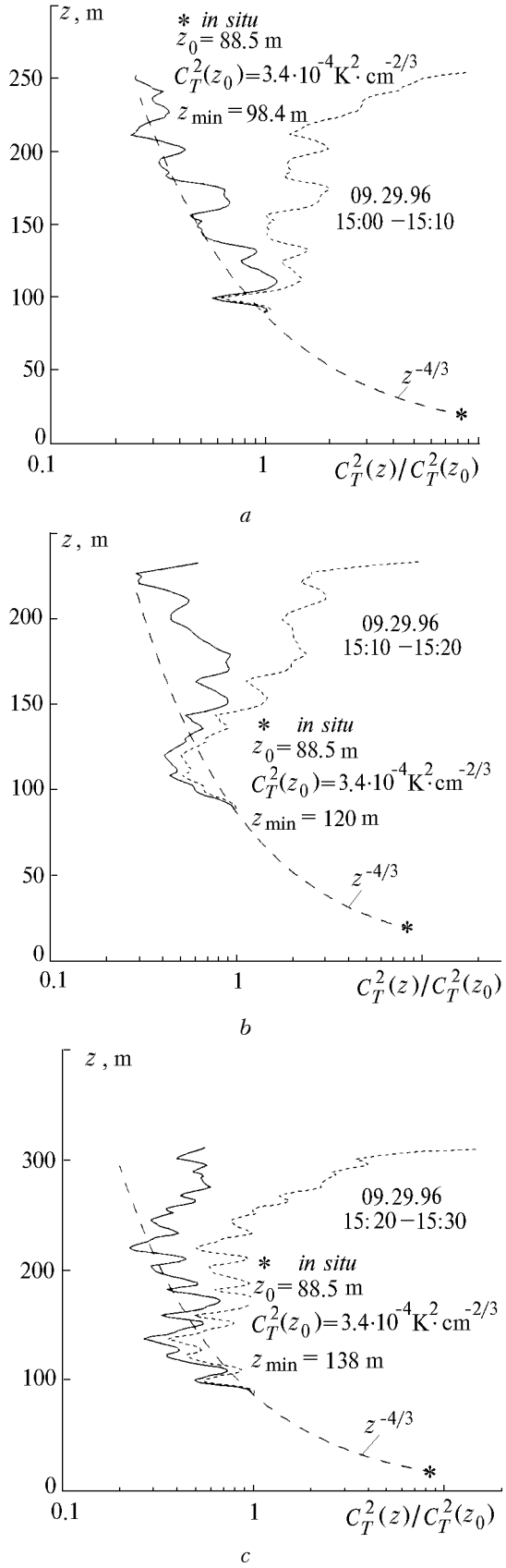

FIG. 2. Normalized vertical profiles of C_T^2 for three subseQuent runs indicated in Fig. 1.

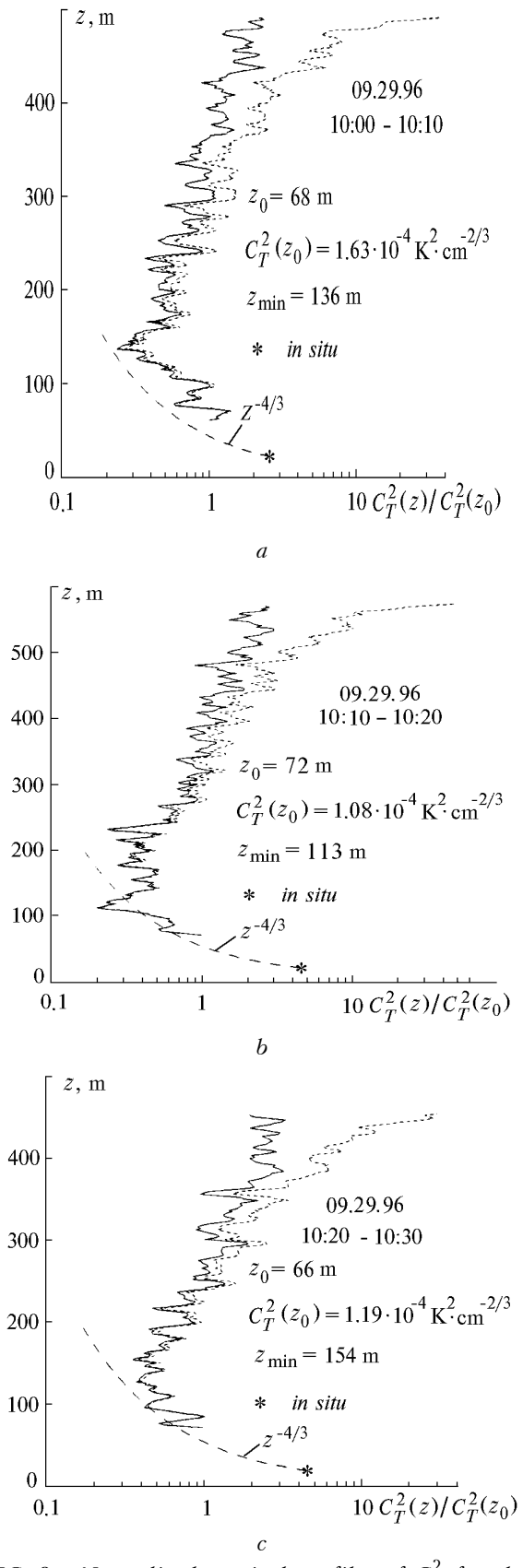

FIG. 3. Normalized vertical profiles of C_T^2 for three subseQuent 10-min runs under conditions of developing convection.

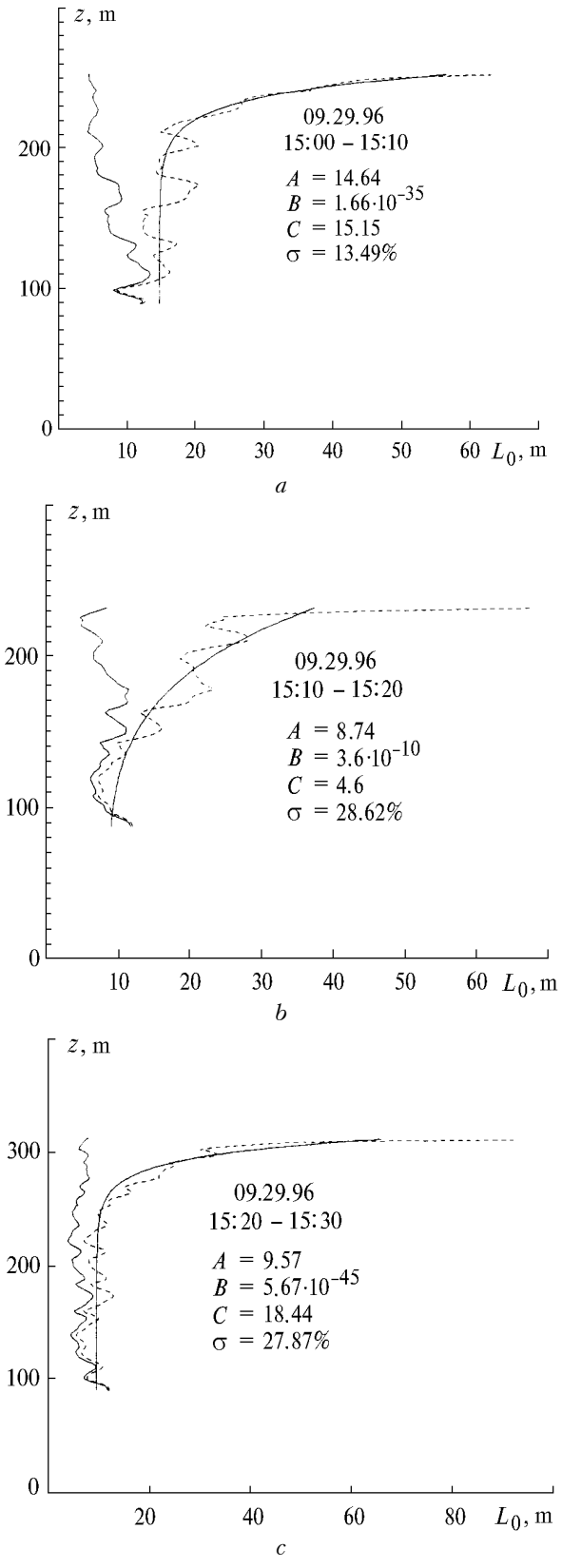

FIG. 4. Vertical profiles of the outer scale of atmospheric turbulence for three subseCuent runs indicated in Fig. 1. The corresponding vertical profiles of C_T^2 are shown in Fig. 2.

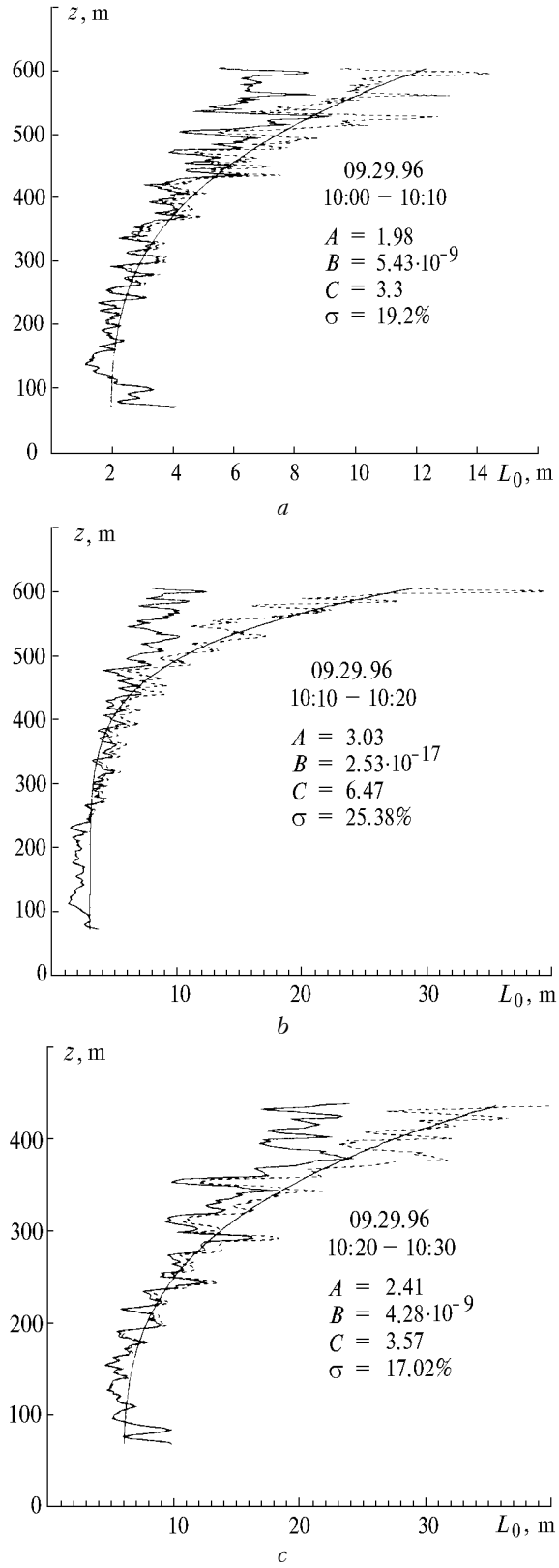

FIG. 5. Vertical profiles of the outer scale of atmospheric turbulence for three-subseCuent 10-min runs on September 29, 1996. The measurements started at 10:00, Tomsk local time, under conditions of developing convection. The corresponding profiles of C_T^2 are shown in Fig. 3.

The solid curves are for the first iteration and the dashed curves are for the last iteration for 5% level of convergence of the algorithm. The long-dashed curve illustrates the dependence $C_T^2(z) \sim z^{-4/3}$ predicted theoretically for convective conditions. All curves reach their minima at $z_{\min}$. Below $z_{\min}$, the behavior of C_T^2 is described well by the theoretically predicted dependence. Above $z_{\min}$ C_T^2 increases with the altitude, which was also indicated in Ref. 7. The asterisks indicate the values of C_T^2 (17 m) calculated from the data of simultaneous measurements with micropulsation sensors.

Considering $z^{-4/3}$ dependence, they agree well with the sodar data.

Figures 4 and 5 show the vertical profiles of L_0 for these runs.

The solid curves show the first iterations and the dashed curves show the last ones. The obtained profiles were approximated by the nonlinear least-squares method using the relation

$$L_0(z) = A + B\, z^C. \qquad (23)$$

The values of the corresponding coefficients and the rms fitting errors δ are also shown in the figures. The smooth solid curves illustrate this empirical dependence.

As can be seen from Figs. 4 and 5, the outer scale of turbulence increases with the altitude. This agrees with the existing models of the outer scale of atmospheric turbulence reviewed in Ref. 13. Its near-ground values A change from 1.98 to 14.68. According to Ref. 13, the effective outer scale of atmospheric turbulence determined by minimization of the integral quadratic discrepancy of the structure functions of the optical wave phase fluctuations corresponding to the model profile of the outer scale $L_0(z)$ and the constant value of the outer scale L_0^* lies between 0.68–34.7 m for the lowest intensity of the atmospheric turbulence corresponding to the best conditions of vision through the atmosphere and between 1.31–55.4 m for the highest intensity of the atmospheric turbulence corresponding to the worst conditions of vision through the atmosphere. It should be noted that the data of sodar measurements are within these limits.

Within the 80–140 m altitude range the vertical behavior of the outer scale shown in Fig. 4*b* follows the dependence $L_0(z) = 2\sqrt{z}$. In Figs. 4*a* and *c*, L_0 remains practically unchanged at altitudes up to 150–200 m. From Fig. 5 it is seen that the outer scale of atmospheric turbulence changes quasiperiodically with a period of 10 min, because the vertical profiles of L_0 shown in Figs. 5*a* and *c* are very similar. That is, in analogy with Refs. 15 and 16, we suggest that 10-min intermittence of atmospheric turbulence (dramatic changes of the low-frequency section of the turbulence spectrum) occurs in the atmosphere.

The fact that in the first run under conditions of developed convection (see Fig. 4) we recorded the most strong echo signals from altitudes up to 550 m has engaged our attention; at that time L_0 = 14.64 m in the lower part of the atmospheric boundary layer (ABL). In the second run, the echo signal was weak and L_0 = 8.74 m in the lower part of the ABL (see Fig. 1). In the third run, the echo signal power increased and L_0 = 9.57 m in the lower part of the ABL.

In conclusion it also should be noted that in the morning under conditions of developing convection we recorded smaller values of L_0, which is in agreement with the experimental data reported in Ref. 14.

ACKNOWLEDGMENT

This material is based upon work supported by the US Government through its European Research Office of the US Army under Contract No. 68171–96–C–9067.

REFERENCES

1. N.P. Krasnenko and L.G. Shamanaeva, Atmos. Oceanic Opt. **10**, No. 2, 129–131 (1997).
2. N.P. Krasnenko and L.G. Shamanaeva, in: *Extended Abstracts of Reports at the COST-76 Profiler Workshop 1997*, Engelberg (1997), Vol. II, pp. 318–321.
3. N.P. Krasnenko and L.G. Shamanaeva, in: *Abstracts of Reports at the Fourth Symposium on Atmospheric and Oceanic Optics,* Tomsk (1997), pp. 160–161.
4. A.N. Kolmogorov, Dokl. Akad. Nauk SSSR **30**, 229 (1941).
5. R.A. Baikalova, G.M. Krekov, and L.G. Shamanaeva, JASA **83**, No. 4, 1332–1335 (1988).
6. M. Sazarin, ed., VLT Report No. 60, European Southern Observatory, La Silla (1990), 71 pp.
7. W.D. Neff, Report ERL 322–WPL **38**, Boulder (1975), 34 pp.
8. V.S. Komarov, *Statistical Structure of the Humidity Field in the Free Atmosphere above the Territory of the USSR* (Gidrometeoizdat, Leningrad, 1971).
9. E.H. Brown and S.F. Clifford, JASA **60**, No. 4, 788–794 (1976).
10. V.I. Tatarskii, *Wave Propagation in a Turbulent Medium* (McGrow-Hill, New York, 1961).
11. C.E. Coulman, J. Vernin, Y. Coquenguiot, and L.L. Cassia, Appl. Opt. **27**, No. 1, 155–160 (1988).
12. L.T. Matveev, *Course of General Meteorology. Atmospheric Physics* (Gidrometeoizdat, Leningrad, 1976) 639 pp.
13. V.P. Lukin, E.V. Nosov, and B.V. Fortes, Atmos. Oceanic Opt. **10**, No. 2, 100–106 (1997).
14. O.N. Emaleev, V.P. Lukin, V.V. Pokasov, and S.F. Potanin, in: *Abstracts of Reports at the Fifth All-Union Symposium on the Propagation of Laser Radiation through the Atmosphere,* Tomsk (1979), pp. 144–147.
15. V.P. Lukin, Atmos. Oceanic Opt. **5**, No. 12, 834–840 (1992).
16. V.P. Lukin, Atmos. Oceanic Opt. **5**, No. 4, 229–242 (1992).